A Study in Search of Interconnection between Surface Parameters and Surrounding Synoptic and Subsynoptic Features

R. Pradhan, U. K. De

Atmospheric Science Research Group, Department of Physics, Jadavpur University, Calcutta 700032, India

and *P.K. Sen*

Department of Mathematics, Jadavpur University, Calcutta 700032, India

Received November 14, 1994; revised January 18, 1995

ABSTRACT

The paper reveals that the variations in parameters like $\bar{u}_*$, the scaling velocity and θ_*. The scaling temperature during the various phases of monsoon might be linked with subsynoptic features. The rise in u_* is mainly connected with the presence of lower tropospheric cyclonic vorticity over a subsynoptic scale of the site. However the variations in θ_* is mainly linked with the various phases of monsoon and θ_* shows a sharp rise in presence of low level convective cloud.

Besides the correlation studies of u and u_*, θ_v and θ_{v*}, $\theta_v - \theta_{v0}$ and θ_{v*} are undertaken. The correlation between θ_v and θ_{v*} is poor. In other two cases correlations are good. Besides $\partial u / \partial u_*$ has shown good coefficient of variation values within the ζ range.

Key words: Scaling velocity, Scaling temperature, Subsynoptic feature, Correlation coefficient, Coefficient of variation

I. INTRODUCTION

The atmospheric boundary layer is the zone, adjacent to the earth's surface where turbulence is induced both by wind and buoyancy and the process is continuous both in time and space scale. The lowermost portion of the layer is called surface layer where the fluxes of momentum, heat and moisture are most dominant. Actually these fluxes may be expressed in terms of surface parameters like the scaling velocity (u_*), the scaling temperature (θ_*) and moisture concentration (q_*). Incidentally the present study deals with u_* and θ_* only. These parameters have been evaluated using established flux–profile and similarity relations of wind and temperature (Paulson, 1970; Dyer, 1974; Kramm, 1989; Pradhan et al., 1994). These two parameters are utilized here to understand the type of convection involved over the observational station which incidentally lies at a deep convective zone. The terminology, free convection is used for convection due to buoyancy only and the convection due to any factor other than buoyancy is termed as forced convection.

The observations regarding u_* and θ_* reported here are derived using the data taken during Monsoon Trough Boundary Layer Experiment, 1990 (MONTBLEX'90). This widespread experiment initiated by the Department of Science and Technology (DST) of Govt. of India was carried out during the monsoon of 1990 covering the entire northern India. In fact, little information was available before this experiment regarding the nature of boundary layer processes going on over the monsoon trough region extending over entire North Indian landscape. In fact, from the location of the trough one can expect the process to vary from near dry, unsaturated to deep moist type over the dimension. The station of present study is incidentally located in a deep moist convective zone. The axis of the sruface pressure trough during SW–monsoon season usually lies parallel to Himalayan foothills with near NW–SE extension. The western end of the trough extends over West Rajasthan where dry convection with shallow clouds is prevalent, on the other hand, the eastern end extends over head Bay of Bengal through the southern part of Gangetic West Bengal (GWB). This situation normally prevails over four months(June–Sept.).

Among the several micrometeorological facilities available during MONTBLEX'90, one 30 m high tower was erected at Kharagpur(KGP) in the state of West Bengal, which lies in the trough region of Gangetic West Bengal (GWB). The surface layer parameters have been evaluated using the available data from the slow response type sensors only, located at various levels and the period of study, is from May 27, 1990 to July 18, 1990. This period extends from Julian day (JD) 147 to 199. The stability condition of the surface layer has been decided only from the thermal stability (Sec. 2.3) and the situation may be divided under two heads, one grouped under stable or neutral (S / N) situation and the other under unstable (US) situation. The accumulated mean value of each situation of a day is taken as the corresponding representative value for that day.

The various features of premonsoon and monsoon activities during the period of May 27 to July 18, 1990 have been derived with the help of working charts available from India Meteorological Department (IMD). For this purpose surface working charts available at 3 hours interval and upper air charts at 6 hours interval have been utilized (Sec. 3.1).

The main theme of the present work is to establish the interconnection between the surface parameters like u_* and θ_* and the various phases of synoptic and subsynoptic features during the concerned period.

II. DATA AND ANALYSIS

1. The surface synoptic data are available at every three hour interval at station Kalaikunda (KKD) of Indian Air Force, which lies within 10 km of KGP station. Incidentally it has been found that the wind speed at anemometer height of 15.3 m and the dry bulb temperature at 1.2 m height of KKD have good correlation with the corresponding data at respective levels of KGP (Table–1). In fact the temperatures are appreciably different for the two different places (Figs. 1 and 3) though the correlation is very high both in US as well as S / N conditions. This departure may be due to interpolation used in Kalaikunda data to generate data in every half an hour interval from real data of 3 hour interval. Moreover the temperature depends sharply on various local factors. Winds at two places have better match in magnitudes (Figs. 2 and 4), with a high correlation both in S / N and US conditions. Thus all the available informations at KKD like present and past weather, rain fall, cloud conditions and the other standard meteorological parameters at 3 hour interval are considered same with the tower site at KGP.

Table 1. Correlation of Wind Speed and Temperature between KGP Tower and KKD Surface Data

Stability	Parameter	R	SMR	P
Unstable	Wind	0.864	0.747	0.0
	Temperature	0.868	0.753	0.0
Stable /	Wind	0.888	0.789	0.0
Neutral	Temperature	0.781	0.611	0.0

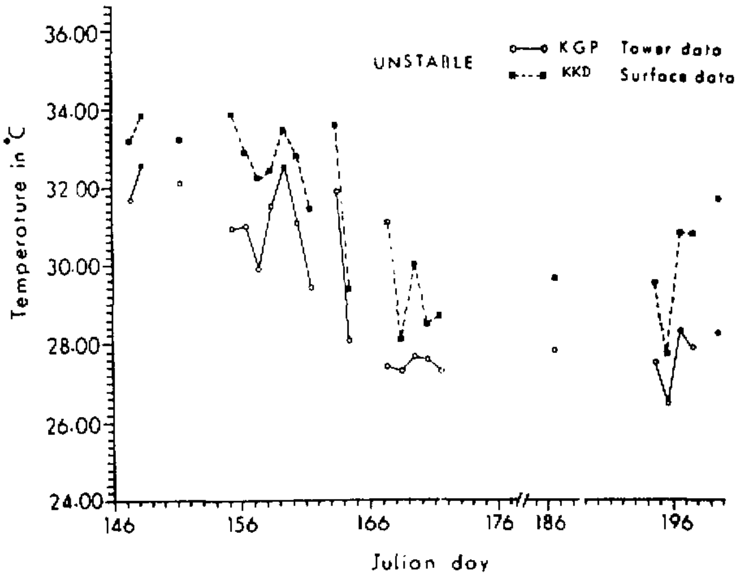

Fig. 1. Comparison of temperature between KGP–tower and KKD–surface data in unstable situation.

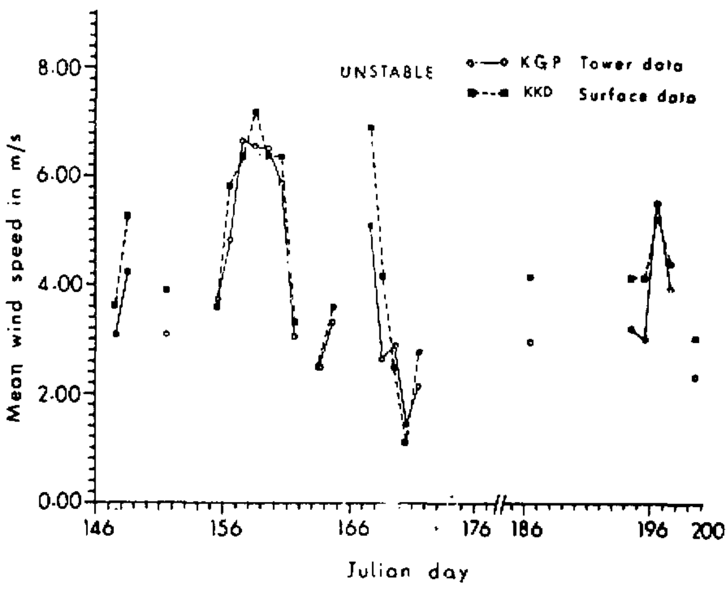

Fig. 2. Comparison of mean wind speed between KGP–tower and KKD–surface data for unstable condition.

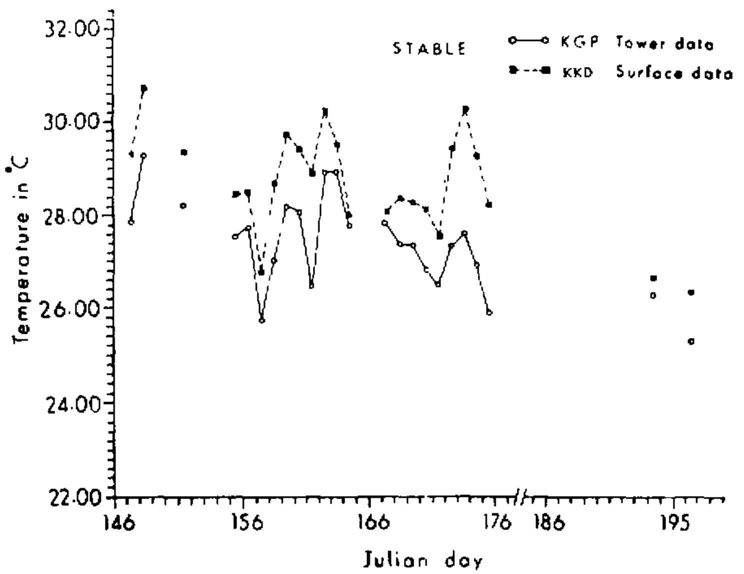

Fig. 3. Comparison of temperature between KGP–tower and KKD–surface data for stable situation.

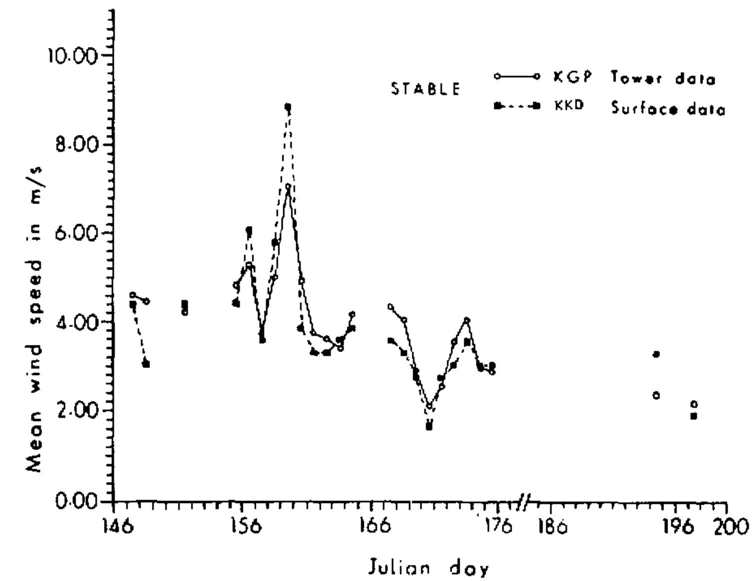

Fig. 4. Comparison of mean wind speed between KGP–tower and KKD–surface data for stable situation.

2. To understand the mesoscale, subsynoptic or synoptic weather phenomena around KGP, the data from the following sources were utilized:

(1) Monthly Meteorological Registers (MMR) of 10 stations in GWB and two stations of Orissa around KGP,

(2) Regional Daily Weather Reports (RDWR) of 1990, issued by the Regional Centre of Calcutta,

(3) Indian Daily Weather Report (IDWR) of 1990, issued by IMD, Pune,

(4) Surface weather charts at three hour interval, available from Regional Centre, IMD, Calcutta.

3. The 30 m micrometeorological tower located at KGP site had six levels of instrumentations at 1 m, 2 m 4 m, 8 m, 15 m and 30 m heights, with both slow and fast response sensors. Though temperature, wind velocity and wind direction sensors of slow response type were located at all six levels the relative humidity sensors were located at 4 levels only (1 m, 4 m, 15 m and 30 m heights). The sampling rate of the sensors was 1Hz and the data were available in general continuously as 3 min average value. However it has been found that 30 min averaging is more suitable in many studies as too many fluctuations are then erased out without disturbing the variational pattern.

In fact there are 53 days from May 27, 1990 to July 18, 1990, but data files are available only for 34 days. In fact beyond July 18, 1990, the data files are highly irregular or scanty. On those 34 days, data files are used to evaluate the surface parameters u_* and θ_* from each half hourly averaged data. The nature of stability is determined on the basis of signature of θ_*. When θ_* is positive as well as has values close to zero (in the range $-0.01 \leqslant \zeta \leqslant 0.01$), the situation is taken as stable or neutral and for all other negative values, the situation is unstable. The accumulated average of surface parameters for a particular situation is taken as the representative value for that particular day. However, the following rules are being followed in order to accept the representative value:

(i) Data must exist for 60% or more of the time of the expected length of stability.

(ii) If the data availability is from 60% to 80% of the expected length of a particular stability, the data discontinuity must not exist continuously for more than one hour of the stability.

(iii) If the data availability is above 80% of the expected length of a particular stability, the maximum data discontinuity for that period is allowable upto 2 hours.

(iv) In case there is any uncertainty about the length of the expected duration of stability, then the data set for that particular stability is not considered at all.

If all the above four criteria are satisfied, but the data for u_* and θ_* are unavailable for any half an hour point, those are recovered using linear interpolation.

Following the above mentioned procedure, the representative data points for 23 days are found to be acceptable in the unstable situation. On 9 occasions, the rejection is applied because the data structure does not satisfy (i) to (iii) of the above mentioned criteria and only on two occasions (JD172, JD173),rejection is applied because of criterion (iv).

Similarly 24 data points are available for the stable or neutral situations. On 10 occasions the data sets fail to come through the criteria (i) to (iii). Only on 1 occasion, data sets fail to come through criterion (iv).

III. OBSERVATIONS AND DISCUSSIONS

1. The Monsoon of 1990 was quite normal according to IMD. The axis of the monsoon pressure trough normally passes through Delhi, Allahabad (Uttar Pradesh), GWB upto the

head of the Bay of Bengal. In the year 1990 it was established to the east of longitude 80°E during the third week of June and beyond that longitude, i.e. over NW India, by the end of June. During the month of July, the trough was in general weak and ill defined. But it revived in those areas of low pressures with its position usually to the south of the normal position.

In fact, during the monsoon of 1990, the typical "Break Monsoon" condition was almost absent. On a few occasions the eastern or the western end of the trough moved close to the foothills of the Himalayas, but this situation incidentally lasted for a very short period.

2. The overall synoptic situation during the monsoon of 1990 has been presented by IMD and the intensive observation periods (IOPs) have been declared by DST. In Table 2, the synoptic situations around GWB as well as IOP–s during the period of present study are being reproduced. In fact any synoptic event beyond 5°of KGP, both in latitude or longitude is not being noted for the present study.

Table 2. IOP–s with Synoptic Features over Eastern End of Trough during 1990 Monsoon

ST. No.	Weather system	Place of 1st location	Period, Direction of movement	Place of dissipation	Remarks	IOP–s
1.	Lower and midtropospheric cyclonic circulation	NW– and adjoining WC–Bay off South Orissa & N–Andhra Pradesh	June 4–7, W'ly	Telengana & neighbourhood		June 1–17 Onset phase i.e., monsoon trough formative stage
2.	Deep depression	NW–Bay	June 13–15 NW / WNW'ly	E–M.P. & adj–B. PLT & Orissa	Initially cy–circulation between 2.1–4.5 km. asl over WC–Bay on 7th	
3.	Well marked low pressure area	B. PLT & its neighbourhood	June 21–30 initially E'ly & then WNW'ly	South U.P. and adj. M.P.	Initially cyclonic circulation over B. PLT neighbourhood	
4.	Lower and mid-tropospheric cyclonic circulation	GWB and neighbourhood	July 1–5 Quasi stationary	GWB and B. PLT	–	July 5–15 Intense convective and trough fluctuating phase
5.	Mid–tropospheric cyclonic circulation	Orissa & adj. GWB & B. PLT	July 6–7 Stationary	In Situ	–	
6.	Lower tropospheric cyclonic circulation	Bangladesh	July 6–10 NE'ly	Assam & neighbourhood	–	
7.	Mid–tropospheric cyclonic circulation	WC–Bay off N–Andhra Pradesh	July 16–23 NW'ly	Central Bihar & adj. U.P.	–	
8.	Low pressure area	GWB and adj. NW–Bay	July–14–17 WNW'ly	NW M.P. & neighbourhood	Initially cyclonic circulation middle tropospheric levels over NW–Bay and adj. GWB	

For the subsynoptic features, use has been made of all the sources reported in Section 2.2. In the following, the important subsynoptic features around the present site and during the period of present study are only being noted down. These essentially supplement the systems noted in Table 2.

(1). Over the synoptic event of June 4–7, an embedded cyclonic circulation developed over GWB and B. PLT. in the afternoon of June 6 and this system persisted upto the morning of June 7.

(2). Though the depression phase lasted from June 13–15, a low pressure developed over West Central Bay and North Andhra Coast from the evening of June 10. Ultimately the depression formed on the night of June 13. Depression intensified and came closest to the station in the morning of June 14. It crossed the land in the afternoon and then became less marked.

(3). Pressure trough was established on June 16 and June 16–17 might be considered as trough establishing phase.

(4). A low pressure system associated with cyclonic circulation and its small fluctuations prevailed over GWB, B. PLT., Orissa and North Bay of Bengal during the period June 19–27. However the system intensified over GWB and B. PLT. on June 24 giving rise to cyclonic circulation from surface to 5.8 km. AGL height. June 19–27 may be considered as active monsoon phase.

(5). A break type situation developed over Eastern India from the afternoon of June 29 to the evening of June 30. A warm core also developed over GWB on the evening of June 30 and with it the surface pressure trough revived.

(6). An embedded lower tropospheric cyclonic circulation appeared over GWB from July 13–15, over the low pressure area extending from GWB TO NW–Bay.

(7). Pressure trough became less marked over GWB during July 16–18.

3. The 23 data points available as representative magnitudes of u_* and θ_* for a day during the unstable situations, are presented in Figs. 5 and 6. In the present study Julian day starts at 0000 IST. How the variations in u_* and θ_* are related with various subsynoptic features and the subsequent remarks are presented through Tables 3 and 4.

Table 3. u_* in Unstable Condition

Variation of u_* during the period	Synoptic event	Remarks
Shoots up during June 6–8	Over the synoptic event of June 4–7, there was embedded cy. cir over GWB and B. PLT. in the afternoon of June 6 and persists upto the morning of June 7.	Whenever there exists a cy. vortex around GWB in subsynoptic scale, u_* rises.
Shows an upward trend from June 13 but data are unavailable for June 14 and 15	This is evidently connected with the depression phase existing June 13–15. Apperently depression had its effect on the station as a subsynoptic phenomena during June 14–15.	u_* is low when trough is established and monsoon is active.
A rise on July 15, though the trend started from July 13. Settles down to a low value on July 18	Connected with lower tropospheric cy. circulation over GWB from July 13–15.	

Table 4. u_* in Stable Condition

Variation of u_* during the period	Synoptic event	Remarks
There is a sharp rise in magnitude on June 8, u_* is high during preonset or onset phase. But value is correspondingly lower during active monsoon phase or trough fluctuating phase.	On June 8, there was strong surface wind, observed over KKD with velocity more than 20 knots. Cyclonic vortex over GWB started dissipation from midday of June 7	Apparently u_* depends much on the magnitude of surface wind velocity.

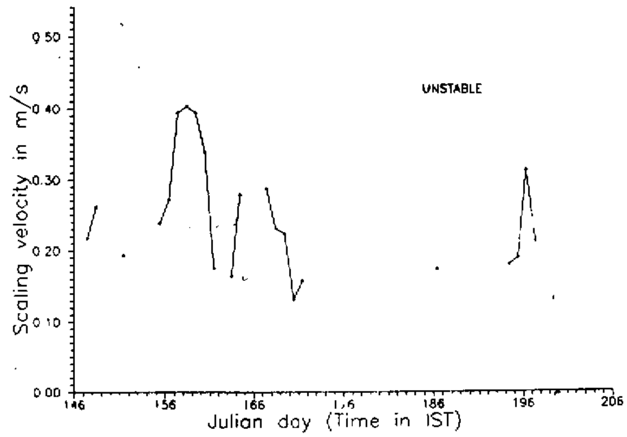

Fig. 5. Time series of daily mean u_* for unstable situation over KGP tower station.

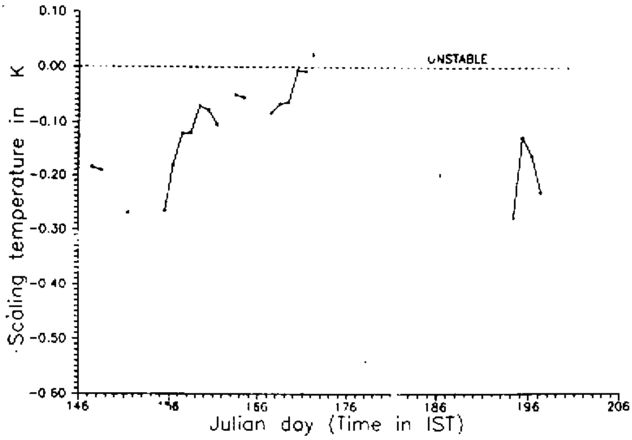

Fig. 6. Time series of daily mean θ_* for unstable situation over KGP tower station.

Similarly 24 data points available for the same quantities in the stable or neutral situation, are presented in Figs. 7 and 8 respectively. The interrelations are now presented through Tables 5 and 6.

4. In the present section, the results of the following correlation studies are being presented; both for US and S / N situation,

(i). between u and u_*

(ii). between ∂u and ∂u_*

(iii). between θ and θ_* on the one hand and between $\theta - \theta_0$ and θ_* where θ_0 is potential temperature at the height of Z_0.

(1) In the US situation, Pearson correlation coefficients between u and u_* in different ranges of ζ and for the entire range of study, $-.01 > \zeta \geqslant -10$ are presented in Table 7. The study is based on half an hour mean value of u and u_*. It is evident that except in the initial range of $-.01 > \zeta \geqslant -0.1$, the correlation coefficient gradually decreases with rise in ζ range. This is understandable, if one looks at the standard flux–profile relationship.

Table 5. θ_* in Unstable Condition

Variation of θ_* during the period	Synoptic event	Remarks
Highest value during the onset phase occurs on June 4 and the value gradually falls off	During June 4–6, there was intense low level cloud over GWB. In the evening of June 4, there was precipitation in presence of convective type clouds. Apparently in its wake the surface temperature dropped on June 5. Again in the night of June 5, there was precipitation and probably this caused further drop in surface temperature. On June 6 there was wide spreaded St cloud. From June 7–9, no low level cloud is being reported by Ceilometer at KKD.	One can concluded that θ_* shows a sharp rise in the presence of low level convective clouds. θ_* might go down under the following situation: i). whenever the cloud is stratiform type. This situation has been observed significantly in active monsoon phase, ii). in presence of poor insolation and iii). in presence of intense rainfall.
θ_* poor during active monsoon phase from June 17	From June 17–29, the monsoon became active and sometimes it turned vigorous over GWB. Due to presence of stratiform clouds buoyancy force weakened, besides the existance of the associated rainfall and poor insolation.	
It has higher value on July 13, then drops on July 14 and again goes on rising and maximum reached on July 18	On July 13, low level convective clouds existed along with the lower tropospheric cyclonic circulation. On July 14, there was intense rainfall. From July 15 and onward the convective cloud reintensified.	

Table 6. θ_* *in Stable Condition*

Variation of θ_* during the period	Synoptic event	Remarks
θ_* moderate during preonset and onset phase and it is maximum on May 31.	This phase is mainly associated with thunderstorm phenomena. May 31 was a thunderstorm day with intense rainfall. So a significant surface stability is expected.	*Subsidence is comparatively* higher during active monsoon phase and poorest in trough fluctuating phase.
θ_* sharply rises during June 21–22.	Surface stability was present throughout the day with a vigorous monsoonal condition.	
θ_* is poorer from July 5–18	During trough fluctuating phase surface layer is relatively less stable due to *convective cloudy condition.*	

Table 7. A Statistical Study Related to u and u_*

Unstable condition				*Stable condition*#			
Range of ζ	% of data	CV % of $\partial u / \partial u_*$	r_{u}, u_*	Range of ζ	% of data	CV % of $\partial u / \partial u_*$	r_{u}, u_*
$-0.01 > \zeta \geqslant -0.1$	32.12	14.24	0.705	$0.01 < \zeta \leqslant 0.1$	50.13	13 57	0.700
$-0.1 > \zeta \geqslant -2$	58.23	06.10	0.919	$0.1 < \zeta \leqslant 2$	45.32	32.93	0.519
$-2 > \zeta \geqslant -5$	05.22	02.76	0.880	$2 < \zeta \leqslant 5$	03.32	41.60	0.439
$-5 > \zeta \geqslant -10$	04.43	11.34	0.670	$5 < \zeta \leqslant 10$	01.23	32.43	0.472
$-0.01 > \zeta \geqslant -10$	100	10.40	0.857	$0.01 < \zeta \leqslant 10$	100	58.10	0.603

Neutral condition is separated out.

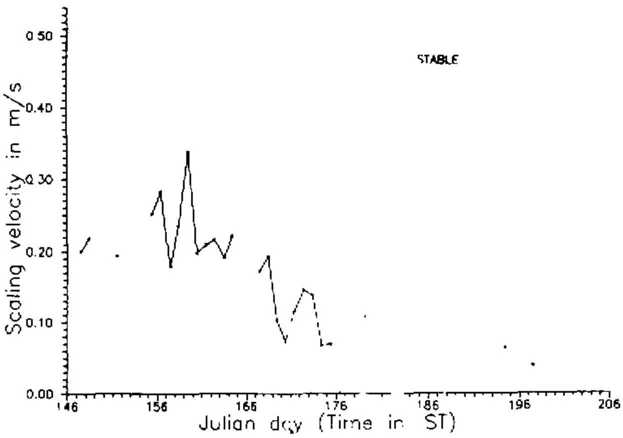

Fig. 7 Time series of daily mean u_* for stable situation over KGP tower station

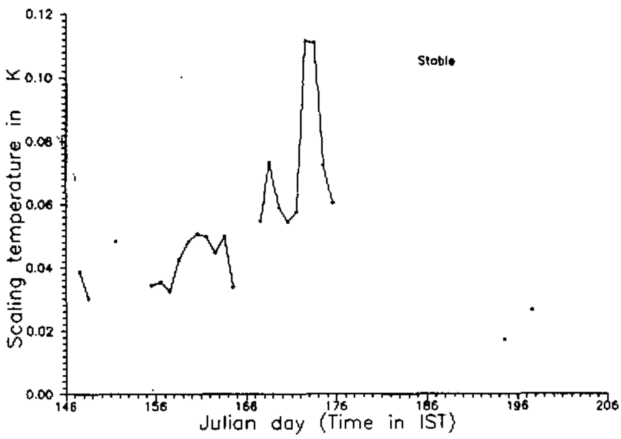

Fig. 8. Time series of daily mean θ_* for stable situation over KGP tower station.

$$u_z = A + BX \tag{1}$$

where

$$A = -B\ln Z_0, \tag{1.1}$$

$$B = u_* / 0.4 \tag{1.2}$$

$$X = \ln Z - \psi_m(\zeta) \tag{1.3}$$

$$\psi_m(\zeta) = 2\ln(1+x)/2) + \ln((1+x^2)/2) - 2\tan^{-1}x + \pi/2, \tag{1.4}$$

$$\zeta = z / L \tag{(1.5)}$$

(Sorbjan,1989).

Here

$$L = \frac{\theta_m u_*^2}{kg(\theta_* + 0.61\theta_m q_*)}. \tag{1.6}$$

Incidentally $\psi_m(\zeta)$ has highly nonlinear relationship with ζ. Inspite of that, one can conclude that for small $|\zeta|$, $\psi_m(\zeta)$ will be small. Then the correlation between u and u_* is expected to be high. This is evident from Table 7.

In fact in the present data set, 90% falls within ζ value of -2. From this, one can expect that some significant contribution of u_* in comparison with θ_*. This is further substantiated by the fact that u_* in the unstable situation hardly falls below 0.1 m / s. Thus the monsoon in GWB is rarely free convective type, rather it should be termed as deep convective type where both u_* and θ_* make significant contributions.

The lower correlation between u and u_* in the range $-0.01 > \zeta \geq -0.1$ compared to the next range, is due to relatively high nonlinear relationship between $\psi_m(\zeta)$ and ζ (Businger et al., 1971).

In the stable case,

$$\psi_m(\zeta) = -5\zeta \tag{1.7}$$

In fact 95% of the data sets in this case, fall within the range $0.01 < \zeta \leq 2$ and as expected, the correlation coefficient gradually falls with rise in ζ value. It should be mentioned that in combined S / N situation, the correlation coefficient rises to 0.914. One can note that $\psi_m(\zeta)$ tends to zero in the neutral case and then correlation becomes very strong and this greatly influences the overall picture.

(2). Using previous relation, one can express

$$\partial u / \partial u_* = \frac{1}{k}[\ln(Z / Z_0) - \psi_m(\zeta)] + 2(1 - 1 / x) \tag{1.8}$$

for the US situation and

$$\partial u / \partial u_* = \frac{1}{k}[\ln(Z / Z_0) - 5\zeta] \tag{1.9}$$

for the stable situation.

The coefficient of variation (CV) of $\partial u / \partial u_*$ given in Table 7, is based on the above two relations. Since CV is low for all discrete ranges as well as for the entire ranges, one can expect good correlation between u and u_*. This is evident by relations summerized in Table 7. Further this is supported by the observed correlation coefficient between Δu and Δu_* which is 0.729 in the unstable situation and 0.702 in the stable situation.

(3). In the US as well as S / N situation, the correlation coefficient between θ and θ_{v*} is always poor. This is 0.228 for US and 0.094 for S / N situations. This can be realized if one looks at the flux–profile relationship for θ and θ_{v*} in the US situation,

$$\theta_v(Z) = C + DY \tag{2}$$

where,

$$C = \theta_{v0} - D \ln Z_0, \tag{2.1}$$

$$D = \theta_{v*} / .4, \tag{2.2}$$

$$Y = \ln Z - \psi_h(\zeta), \tag{2.3}$$

$$\psi_h(\zeta) = 2\ln(1 + x^2) / 2) \tag{2.4}$$

Here,

$$\psi_h(\zeta) = -5\zeta \tag{2.5}$$

for stable situation and

$$\psi_h(\zeta)=0 \tag{2.6}$$

for neutral situation.

In fact, as θ_v changes θ_{v0} which is the magnitude of θ_v at $Z=Z_0$, the roughness length, also changes. Thus θ_{v*} is expected to be more dependent on the difference between θ_v and θ_{v0}, rather than θ_v itself. This is corroborated by the high correlation coefficient between $(\theta_v-\theta_{v0})$ and θ_{v*} which is 0.96 in US situation.

The line of argument is similar for the stable situation and it turns out that the corresponding correlation coefficient is 0.88 in stable situation. Of course in the present study directly measured θ_{v0} is not available. So model value of θ_{v0} is taken into account.

IV. CONCLUSION

The present study shows that the surface parameters like u_* and θ_* are related more with subsynoptic features than the synoptic features. However θ_* value in stable condition is apparently influenced greatly even by mesoscale features like local thunderstorm phenomena.

Of the two surface parameters the nature of conection between u_* and the subsynoptic features is more understandable. In fact a high value in u_* in the unstable situation is closely linked with the presence of a cyclonic vortex in subsynoptic scale. Besides u_* and u have high correlation in both stable and unstable condition. This shows that u_* is significantly dependent on surface wind.

In fact the nature of relation between θ_* and the synoptic or subsynoptic features is not so clear. Still it is found that the rise in θ_* in unstable condition greatly depends on the presence of low level convective clouds. Significantly low value has been observed in presence of stratiform clouds. It is also to be noted that θ_{v*} and θ_v are rather poorly correlated though $\theta_v-\theta_{v0}$ and θ_{v*} have high correlation.

The author's thanks are due to Dept. of Science and Technology, Govt. of India, for the sanction of a research project and the present work is a part of that project. The authors also wish to express thanks to India Meteorological Department, Indian Air Force, Govt. of India, for helping with necessary data.

REFERENCES

Businger J.A. Wyngaard J.C., Izumi Y. and Brodley E.F. (1971), Flux–Profile Relationship in the Atmospheric Surface Layer, *J. Atmos. Sci.*, **28**: 181–189.

Dyer A.J. (1974), A Review of Flux–Profile Relationships, *Boundary Layer Meteorology*, **7**: 363–372.

Kramm G. (1989), The Estimation of the Surface Layer Parameters from Wind Velocity, Temperature and Humidity Profiles by Least Squares Method, *Boundary Layer Meteorology*, **48**: 315–327.

Paulson C.A. (1970), The Mathematical Representation of Wind Speed and Temperature Profile in the Unstable Atmospheric Surface Layer, *Journal of Applied Meteorology*, **9(6)**: 857–861.

Pradhan R., De U.K. and Sen P.K. (1994), Surface Sensible Heat Flux Over a Deep Moist Convective Region and Its Interplay With Synoptic and Mesoscale Features, *Proc. Indian Acad. Sci. (Earth and Planetary Sc.)*, **103(3)**: 353–367.

Sorbjan J. (1989), *Structure of the Atmospheric Boundary Layer*, Prentice Hall, Englewood Cliff, New Jersey 07632.